

# Large equivalent width Lyman- $\alpha$ line emission at $z=4.5$ : young galaxies in a young universe?

Sangeeta Malhotra<sup>1,2,3</sup>

and

James E. Rhoads<sup>3</sup>

## ABSTRACT

The Large Area Lyman Alpha survey has found  $\approx 150$  Lyman- $\alpha$  emitters at  $z=4.5$ . While stellar models predict a maximum Lyman- $\alpha$  equivalent width (EW) of  $240 \text{ \AA}$  60% of the Lyman- $\alpha$  emitters have EWs exceeding this value. We attempt to model the observed EW distribution by combining stellar population models with an extrapolation of Lyman break galaxy luminosity function at  $z=4$ , incorporating observational selection effects and Malmquist bias. To reproduce the high EWs seen in the sample we need to postulate a stellar initial mass function (IMF) with extreme slope  $\alpha = 0.5$  (instead of 2.35); zero metallicity stars; or narrow-lined active galactic nuclei. The models also reveal that only 7.5-15% of galaxies need show Lyman- $\alpha$  emission to explain the observed number counts. This raises the possibility that either star-formation in high redshift galaxies is episodic or the Lyman- $\alpha$  galaxies we are seeing are the youngest 7.5-15% and that Lyman- $\alpha$  is strongly quenched by dust at about  $10^7$  years of age.

*Subject headings:* galaxies: general, galaxies: evolution, galaxies: formation, galaxies: statistics, cosmology: observations

## 1. Introduction

Nascent galaxies undergoing their first major burst of star formation are expected to contain many hot, young, massive stars, which ionize interstellar gas. Under standard conditions (case B), about two Lyman- $\alpha$  photons are produced for every three ionizing photons

---

<sup>1</sup>Johns Hopkins University, Charles and 34th Street, Bloomberg center, Baltimore, MD 21218

<sup>2</sup>Hubble Fellow

<sup>3</sup>Space Telescope Science Institute, 3700 San Martin Drive, Baltimore, MD 21218

from the stars. Thus Lyman- $\alpha$  photons can be a prominent signpost of primordial galaxies in formation (Partridge & Peebles 1967, hereafter PP67).

Based on these predictions a number of surveys have been carried out for about three decades (see Pritchet 1994 for a review), with little success until recently. We have recently undertaken a Large Area Lyman Alpha survey (Rhoads et al 2000) to identify a large sample of Lyman- $\alpha$  emitting galaxies at high redshift ( $z = 4.5 \pm 0.1$ ) through narrowband imaging, and so characterize empirically star and galaxy formation in the early universe. Both our survey (Rhoads et al. 2000) and other recent searches over smaller volumes (Cowie & Hu 1998, Hu et al 1998, Kudritzki et al 2000, Fynbo & Moller 2001...others...Pentericci et al. 2001, Stiavelli et al. 2001) are indeed finding high redshift Lyman- $\alpha$  sources, albeit factors of  $\sim 100$  fainter than the early predictions (Partridge & Peebles 1967). This faintness is consistent with the 30 years of nondetections (1967-1997) by many groups that preceded the current generation of searches.

Low luminosity of this line could be due to smaller masses of the sources, lower star-formation rates, or selective obscuration of the resonantly scattered Lyman- $\alpha$  line (Charlot & Fall 1993). The latter scenario would lead to smaller equivalent width (EW) of the line. The EW of the Lyman- $\alpha$  line can also, in principle, be used as a diagnostic to determine the population of young, massive stars. However, this is complicated by several factors: Ionizing flux depends on stellar metallicity; active galactic nuclei may contribute to the ionizing flux; and resonant scattering of the Lyman- $\alpha$  line can make it more sensitive to dust than the adjoining continuum, but (depending on clumping and winds in the interstellar medium) need not do so (Neufeld 1991; Kunth et al 1998).

In this paper we report on the distribution of equivalent widths of Lyman- $\alpha$  line for sources detected in the LALA survey. In section 2.1, we will discuss briefly the LALA survey and selection criteria for sources. Section 2.2 describes how we calculate the equivalent width of the Lyman- $\alpha$  line and presents the observed distribution. Section 3 contains details of stellar population modelling, and section 4 contains discussions and conclusions.

## 2. Observations and equivalent widths

### 2.1. Survey and data reduction

An efficient search for Lyman- $\alpha$  emitters (and other emission line galaxies) was started in 1998 using the CCD Mosaic Camera at the Kitt Peak National Observatory's 4m Mayall telescope. The Mosaic camera has eight  $2048 \times 4096$  chips in a  $4 \times 2$  array comprising a  $36' \times 36'$  field of view. The final area covered by the LALA survey is 0.72 square-degrees in

two MOSAIC fields centered at 14:25:57 +35:32 (2000.0) and 02:05:20 -04:55 (2000.0). Five overlapping narrow band filters of width  $\text{FWHM} \approx 80 \text{ \AA}$  are used. The central wavelengths are 6559, 6611, 6650, 6692, and 6730  $\text{\AA}$ , giving a total redshift coverage  $4.37 < z < 4.57$ . This translates into surveyed comoving volume of  $7.4 \times 10^5$  comoving  $\text{Mpc}^3$  per field for  $H_0 = 70 \text{ km s}^{-1} \text{ Mpc}^{-1}$ ,  $\Omega_M = 0.3$ ,  $\Omega_\Lambda = 0.7$ .

In this paper we report on the data from the spring field centered at 14:25:57 +35:32 (2000.0), since all the imaging on this field at  $z \approx 4.5$  is complete. In about 6 hours per filter per field we achieve line detections of about  $2 \times 10^{-17} \text{ erg cm}^{-2} \text{ s}^{-1}$ . The survey sensitivity varies with seeing. Broadband images of these fields in a custom  $B_w$  filter ( $\lambda_0 = 4135 \text{ \AA}$ ,  $\text{FWHM} = 1278 \text{ \AA}$ ) and the Johnson-Cousins  $R$ ,  $I$ , and  $K$  bands were taken as part of the NOAO Deep Widefield Survey (Jannuzi & Dey 1999).

The images were reduced using the MSCRED package (Valdes & Tody 1998; Valdes 1998) in the IRAF environment (Tody 1986, 1993), together with assorted custom IRAF scripts. Details of the data reduction can be found in the paper by Rhoads et al (2000). Catalogs were generated using the SExtractor package. Fluxes were measured in  $2.32''$  (9 pixel) diameter apertures, and colors were obtained using matched  $2.32''$  apertures in registered images that had been convolved to yield matched point spread functions. In order to gracefully handle sources that are not detected in all filters, we have chosen to use “asinh magnitudes” (Lupton, Gunn, & Szalay 1999), which are a logarithmic function of flux for well detected sources but approach a linear function of flux for weak or undetected sources. The color scatter achieved for bright sources ( $R < 22$ ) is 0.10 magnitudes (semi-interquartile range). This includes the true scatter in object colors, and is therefore a firm upper limit on the scatter introduced by any residual systematic error sources, which we expect to be a few percent at worst.

## 2.2. Selection Criterion

The candidates are selected in the narrow-bands with a detection threshold of  $5\sigma$ , where  $\sigma$  is the root-mean-square (rms) noise determined locally. To reduce the number of foreground [OII] and [OIII] interlopers, we set the minimum observed equivalent width,  $\text{EW} > 80 \text{ \AA}$ . Also, the narrowband flux density should exceed the broad band flux density at the  $4\sigma$  confidence level for a source to be selected as an emission line source. All these criteria are designed to keep the numbers of false candidates down to an acceptable level (Rhoads 2000). An additional condition that the sources not be detected in B-band image selects against low-redshift sources, and is roughly equivalent to a photometric redshift. These criteria yield 157  $z=4.5$  Lyman- $\alpha$  candidates in the three non-overlapping filters  $\text{H}\alpha 0$ ,

H $\alpha$ 8, H $\alpha$ 16.

### 2.3. Equivalent width calculation:

The equivalent width is calculated using narrow and broad band photometry. The observed equivalent width is given by  $EW_o = F_{Ly\alpha}/f_\lambda = (W_R \times N - W_N \times R)/(R - N)$ , where  $F_{Ly\alpha}$  is the flux of the Lyman $\alpha$  line,  $f_\lambda$  is the flux density of the continuum,  $W_N$  and  $W_R$  are widths of the R band (1568 Å) and the narrow-bands (80 Å) respectively, and  $R$  and  $N$  are the respective fluxes in the R-band and the narrow-band in which the source is detected.

The measured equivalent widths are also affected by Lyman- $\alpha$  forest absorption, which can lower both the R-band flux and the line flux. The correction factor for intergalactic absorption is estimated using the prescription of Madau 1995. For the broad band, this is  $\mathcal{A} = 0.58$ – $0.68$  for  $z = 4.57$ – $4.37$ . For a Lyman- $\alpha$  line that is symmetric about zero velocity, we find  $\mathcal{A} = 0.64$ . Thus, the two corrections approximately cancel. The rest-frame equivalent width is then given by  $EW = EW_o/(1 + z)$ . The division by  $(1+z)$  corrects for Hubble expansion.

Figure 1 shows the cumulative distribution of rest-frame equivalent widths after correcting for absorption by the Lyman- $\alpha$  forest. The equivalent widths are derived using equation 1. The continuum is not detected in approximately half the sources. For such sources we use the actual measured R flux at the location of the narrowband source, which makes the equivalent width formally negative in many cases. All such sources are placed in the last bin of the histogram. The median of the distribution is then 400 Å. Figure 1 also shows the cumulative distribution of EWs if we add 1 and 2  $\sigma$  to the R-band flux. Some estimate of the uncertainties in the measurement of the EW can be had from comparing the the three distributions.

## 3. Modelling the distribution of equivalent widths

The equivalent width of the Lyman- $\alpha$  line from stellar systems depends on many factors: the fraction of ionizing photons absorbed by the gas, the dust content of the interstellar medium (ISM), and the relative numbers of ionizing and non-ionizing photons in the UV. The last depends on the slope of the stellar initial mass function (IMF), metallicity of the stellar population, and age of the system. So we know the presence of dust decreases the equivalent width of the Lyman- $\alpha$  line, while metal poor and more massive, young stars

increase it. Charlot & Fall (1993) and Kudritzki et al. (2000) have calculated the Lyman- $\alpha$  equivalent width for stellar populations with different properties.

Our approach here is to combine the luminosity function of galaxies at high redshift with stellar population models and simulate the observational biases reasonably to model the observed Lyman- $\alpha$  emitter population. Since we have a reasonably large sample of Lyman- $\alpha$  emitters, we can use the distribution of equivalent widths as well as the total numbers of such objects as constraints on the nature of these objects.

Three main elements go into modelling the observed number and distribution of equivalent widths:

(1) The luminosity function of galaxies at  $z=4.5$ : Since LAEs are selected on the basis of a strong line this sample can, and does, explore the faint end of the luminosity function (Fynbo et al. 2001). I.e. we can pick up objects with sub-detection level broad-band fluxes and bright emission lines. And as long as the luminosity function is such that there are more faint sources than bright, selection on the basis of line luminosity will result in bias towards high equivalent width sources.

To model the effects of such biases and to explore the relation between line- and continuum-selected high redshift sources, we use the luminosity function of Lyman Break Galaxies (LBGs) at  $z=4.0$ , which is consistent with the faint end luminosity function from the Hubble Deep Field (Pozzetti et al. 1998, Steidel et al. 1999). Translating the luminosity function to a cosmology with  $H_0 = 70, \Omega_M = 0.3, \Omega_\Lambda = 0.7$  at redshift  $z = 4.5$ , we get a Schechter function with  $\phi_* = 1 \times 10^{-3} Mpc^{-3}/mag$ ,  $\alpha = -1.6$  and  $M_* = 25.17$ .

(2) Stellar population modelling: We estimate the equivalent width of the Lyman- $\alpha$  line using the stellar population modelling program “Starburst99” (Leitherer et al. 1999).

The models were run for continuous star-formation. The stellar Initial Mass Function (IMF) is assumed to be a power law with the exponent ranging between  $\alpha = 0.5 - 2.35$ , the latter being the Salpeter law. The metallicity range was from solar to 1/20th solar. Upper mass cutoff was varied between  $M_{upper} = 40 - 120M_\odot$ . For simplicity we consider three models: Model (A) consists of continuous star-formation with Salpeter IMF,  $Z = 1/20$ th solar and  $M_{upper} = 120M_\odot$ . In Model (B) we take the most extreme IMF we dare and set  $\alpha = 0.5$ . Model (C) consists of a zero metallicity stellar population with IMF slope  $\alpha = 2.35$  whose spectra at the age of  $10^6$  years is derived by Tumilinson & Shull (2000). The shape of the age-EW distribution is assumed to be the same as for model (A) since  $\alpha = 2.35$  is the same.

The continuum level at 1225 Å is given directly by the models. The line strength is

derived by assuming that all the ionizing flux is absorbed by neutral hydrogen and produces 2 Lyman- $\alpha$  photons per 3 ionizing photons (case B). We assume that dust absorption and resonance scattering have no effect. All this maximizes the Lyman- $\alpha$  output from galaxies. The equivalent width of Lyman- $\alpha$  is highest when the galaxies are young and asymptotically approaches a steady state value by age  $10^7$  years as seen in Figure 2 (see also Charlot and Fall 1993). For Model C we know the value of EW of Lyman- $\alpha$  at  $10^6$  year but not the evolution of the stellar populations, so we scale the age vs EW curve for model (A) to produce an Lyman- $\alpha$  EW of  $1122 \text{ \AA}$  at  $10^6$  years, since the shape of the age vs EW curve should depend mostly on the IMF slope  $\alpha$ .

The Lyman- $\alpha$  equivalent width distribution of the galaxy population is dependent on the age distribution. In this paper we assume as our null hypothesis that the formation of galaxies is at these epochs is continuous and uniform in time, which is to say there is no special synchronization of galaxy formation better than  $10^8$  years. The consequence of this assumption is that there should be 100 times as many galaxies of age  $10^8$  as  $10^6$ <sup>4</sup>. Therefore the typical equivalent width of the sample should be the equivalent width of galaxies that are  $10^8$  years old, with a tail extending to the highest equivalent width for very young galaxies.

(3) Observational selection effects: Since objects are selected on the basis of having  $5\sigma$  flux in the narrow-band and no restriction in the broad, the error in equivalent widths is dominated by the measurement errors in broad-band flux. In about half the sample the continuum is undetected in the broad band R filter at  $2\sigma$ . Underestimate of the R-band flux can easily push up the EW estimates. So we model the effects of R-band measurement errors on the equivalent width distribution.

Sky noise is the dominant source and is estimated by placing random apertures on the sky. We take the distribution of fluxes measured in  $10^4$  random apertures that satisfy one of the conditions of Lyman- $\alpha$  candidate selection, namely that there be no detectable Bw-band flux. The distribution of fluxes in such apertures is then taken as the empirical distribution of errors in the R-band flux and shows a higher tail than a gaussian distribution.

(4) The Inter Galactic Medium: The R-band flux is reduced due to IGM absorption blueward of the Lyman- $\alpha$  line. We use the prescription by Madau (1995) to calculate the reduction in R-band flux due to the absorption of continuum. The Lyman- $\alpha$  line flux is also reduced due to absorption by galactic and inter-galactic gas, leading to the asymmetric line profile observed in these sources (Rhoads et al. 2000, Rhoads et al. 2001, Malhotra et al.

---

<sup>4</sup>We use age distribution  $0.5 \times 10^6 - 10^8$  years. The upper limit is partly motivated by the age estimates of Lyman Break Galaxies whose luminosity function we use and partly by the age of the universe which is  $\sim 10^9$  years at  $z=4.5$

2001). Reducing the Lyman- $\alpha$  line flux by a factor of 2 is a reasonable approximation (the IGM alone absorbs 36% of the line (Madau 1995)).

Equivalent width ( $EW = f_{Ly-\alpha}/f_\lambda$ ) is not the best formalism to model in a situation where R-band continuum is not detected in half of the sources and flux density  $f_\lambda$  is unknown. Instead of modelling equivalent widths, we work with the ratio of broad-band to narrow-band fluxes  $\Gamma = F_\lambda(R)/F_\lambda(N)$ . With the more uncertain (and small) quantity in the numerator instead of the denominator, the errors are much better behaved. Figure 3 shows the histogram of observed  $\Gamma$  vs  $\Gamma$  in some of the models.

Another advantage of this formalism is that in spite of the many elements that go into reproducing the  $\Gamma$  distribution, these elements are roughly separable in their effects on the distribution. With that in mind we draw the following robust conclusions

- (1) The total number of Lyman- $\alpha$  sources is dependent mostly on the luminosity function. We predict the total number of faint galaxies by extrapolating the LBG luminosity function to lower magnitudes. Only 7.5-15% of these galaxies need to show Lyman- $\alpha$  emission to match the number of Lyman- $\alpha$  emitters found at  $z=4.5$ .
- (2) The median of  $\Gamma$  is unaffected by the noise in R-band flux, which merely broadens the distribution of  $\Gamma$ . The median  $\Gamma = 0.0814$ , which corresponds to an EW of 430 in the Lyman- $\alpha$  line.
- (3) The width of the  $\Gamma$  distribution gives a measure of the scatter in intrinsic value of  $\Gamma$  as well as the flux errors in the R-band. We find that the latter is the dominant contributor to the width of the distribution.

Figure 3 shows how the three models compare with the observed distribution of  $\Gamma$ . We see that none of the models fits perfectly. Model A clearly produces a higher  $\Gamma$  (lower EW) than observed, and is most clearly disfavored. Models (B) and (C) reproduce the median  $\Gamma$  but do not fully account for the width of the distribution. The observed numbers of Lyman- $\alpha$  sources requires that a fraction of faint galaxies show Lyman- $\alpha$  emission. This fraction is 15%, 8.5% and 7.5% for Models (A), (B) & (C)

#### 4. Discussion and conclusions

With Lyman- $\alpha$  sources we are exploring the faint end of the luminosity function, because selection on the basis of line luminosity pulls in sources not easily detected in continuum (Fynbo et al. 2001). Are we also exploring the youngest set of galaxies by selecting them on the basis of their Lyman- $\alpha$  emission? In this paper we have tried to answer that question by studying the equivalent width distribution of these sources. The median equivalent width of

the population is too large to be explicable by ordinary stellar populations. The distribution of equivalent widths can be reasonably (though not perfectly) explained by postulating an IMF that favors more massive stars, or a zero metallicity population. Neither of these scenarios completely explains the low EW tails of the distribution. These tails could be due to more evolved galaxies where dust effects begin to be observable. Since the errors in R-band fluxes are responsible for much of the observed spread in EW, we need deeper R-band images to see the real spread in EW better.

The number of Lyman- $\alpha$  sources is 7.5-15 % of the numbers expected by extrapolating the luminosity function of Lyman Break Galaxies. Perhaps this is a clue that we are only seeing the youngest galaxies and therefore skewed to-towards high EW of Lyman- $\alpha$  line. Why then, do we not see older galaxies with intermediate EWs in our sample? We are sensitive to  $EW > 80/(1+z)$ . Perhaps dust formation after  $10^7$  years quenches the Lyman- $\alpha$  line completely, due to resonance scattering. In another possible scenario, perhaps the early star-formation in galaxies is episodic, so we only see the galaxies when the star-formation episode is less than  $< 10^7$  years old. That is also when the galaxies are brighter. This scenario is also consistent with the blotchy appearances of high redshift galaxies if the different episodes happen in different parts of a galaxy (e.g. Colley et al. 1996).

The high equivalent widths can also be a signature of quasar activity. If so, most of them have to be narrow-line quasars, otherwise we should see the Lyman- $\alpha$  line emission span more than one 80 Å filter. Some of the Lyman- $\alpha$  sources could be type II quasars like the ones found by Norman et al. 2001 & Stern et al. 2001. Chandra deep field observations (Rosati et al. 2001) show that there are  $\approx 2-3 \times 10^3$  x-ray sources per square degree at x-ray fluxes corresponding to the Lyman- $\alpha$  flux limit of our sample. (The x-ray to Lyman- $\alpha$  ratio is fixed using the Norman et al. object). Thus, if all the Lyman- $\alpha$  sources were type II quasars we would violate the X-ray background constraints by a factor of 4-5 unless there were no contribution from the X-ray background from redshifts  $z < 4$  or  $z > 5$ . This is unphysical and contradicts the observed distribution of X-ray source redshifts: The Chandra Deep Field redshift distribution peaks at  $z = 0.7 - 0.8$  and contains no  $z > 4$  sources (Gilli et al. in preparation).

To conclude, this paper reports on the EW distribution of Lyman- $\alpha$  emitting galaxies at  $z=4.5$  and  $5.7$ . The high median equivalent width of the distribution requires that the galaxies be very young, have zero metallicity or stellar IMF of slope  $\alpha = 0.5$ . AGNs can also produce high EWs. If so, we should be able to detect them with the current generation of X-ray observatories. High EWs observed in a large sample obtained by the LALA survey are harder to explain than individual objects (e.g. Ellis et al. 2001), and therefore pose questions that will help us understand galaxy and star-formation in a young universe.



This work made use of images provided by the NOAO Deep Wide-Field Survey (NDWFS; Jannuzi and Dey 1999), which is supported by the National Optical Astronomy Observatory (NOAO). NOAO is operated by AURA, Inc., under a cooperative agreement with the National Science Foundation. We thank Buell Jannuzi, Arjun Dey, and the rest of the NDWFS team for making their images public; and Richard Green and Jim De Veny for their support of the LALA survey. We thank Colin Norman and Tim Heckman for discussing a number of scenarios to explain these observations. JER's research is supported by an Institute Fellowship at The Space Telescope Science Institute (STScI). SM's research funding is provided by NASA through Hubble Fellowship grant # HF-01111.01-98A from STScI. STScI is operated by the Association of Universities for Research in Astronomy, Inc., under NASA contract NAS5-26555.

## REFERENCES

- Bertin, E. and Arnouts, S., 1996, *A&AS* 117,393
- Colley, W. N., Rhoads, J. E., Ostriker, J. P., & Spergel, D. N. 1996, *ApJ*, 473, L63
- Cowie, L. L., & Hu, E. M. 1998, *AJ* 115, 1319
- Charlot, S. & Fall, S. M. 1993, *ApJ*, 415, 580
- Dey, A., Spinrad, H., Stern, D., Graham, J. R., & Chaffee, F. H. 1998, *ApJ*, 498, L93
- Ellis, R. et al. 2001, astro-ph/0109249
- Fynbo, J. U., Möller, P., & Thomsen, B. 2001, *A&A*, 374, 443
- Gilli, R. et al. 2001, in preparation
- Hu, E. M., Cowie, L. L., & McMahon, R. G. 1998, *ApJ* 502, L99
- Jannuzi, B. T., & Dey, A., 1999, in "Photometric Redshifts and High Redshift Galaxies", ASP Conference Series, Vol. 191, editors R. J. Weymann, L. J. Storrie-Lombardi, M. Sawicki, and R. J. Brunner, p.111
- Kunth, D., Mas-Hesse, J. M., Terlevich, E., Terlevich, R., Lequeux, J., & Fall, S. M. 1998, *A&A* 334, 11
- Kudritzki, R.-P. et al. 2000, *ApJ*, 536, 19
- Leitherer, C. et al. 1999, *ApJS*, 123, 3
- Lupton, R. H., Gunn, J. E., & Szalay, A. S. 1999, *aj* 118, 406.
- Madau, P. 1995, *ApJ*, 441, 18
- Neufeld, D. A. 1991, *ApJ*, 370, L85

- Norman, C et al. 2001, astro-ph/0103198
- Partridge, R.B. & Peebles, P.J.E. 1967, ApJ, 147, 868
- Pentericci, L. et al. 2000, A&A, 361, L25
- Pozzetti, L., Madau, P., Zamorani, G, Ferguson, H. C., & Bruzual, G. A. 1998, MNRAS, 298, 1133
- Pritchett, C. J. 1994, PASP 106, 1052
- Rhoads, J. E. 2000, PASP in press (May 2000 issue)
- Rhoads, J. E., Malhotra, S., Dey, A., Stern, D., Spinrad, H., & Jannuzi, B. T. 2000, ApJ, 545, L85
- Rosati, P. et al. 2001, astro-ph/0110452
- Steidel, C. C., Adelberger, K. L., Giavalisco, M., Dickinson, M., & Pettini, M. 1999, ApJ, 519, 1
- Stern, D. et al. 2001, submitted
- Stiavelli, M., Scarlata, C., Panagia, N., Treu, T., Bertin, G., & Bertola, F. 2001, ApJ, 561, L37
- Tody, D. 1993, ADASS II, A.S.P. Conference Ser., Vol 52, eds. R.J. Hanisch, R.J.V. Brissenden, & J. Barnes, 173
- Tumlinson, J. & Shull, J. M. 2000, ApJ, 528, L65
- Valdes, F., & Tody, G. 1998, Proceedings of SPIE Vol. 3355
- Valdes, F. 1998, ADASS VII, ASP Conf. Series 145, ed. R. Albrect

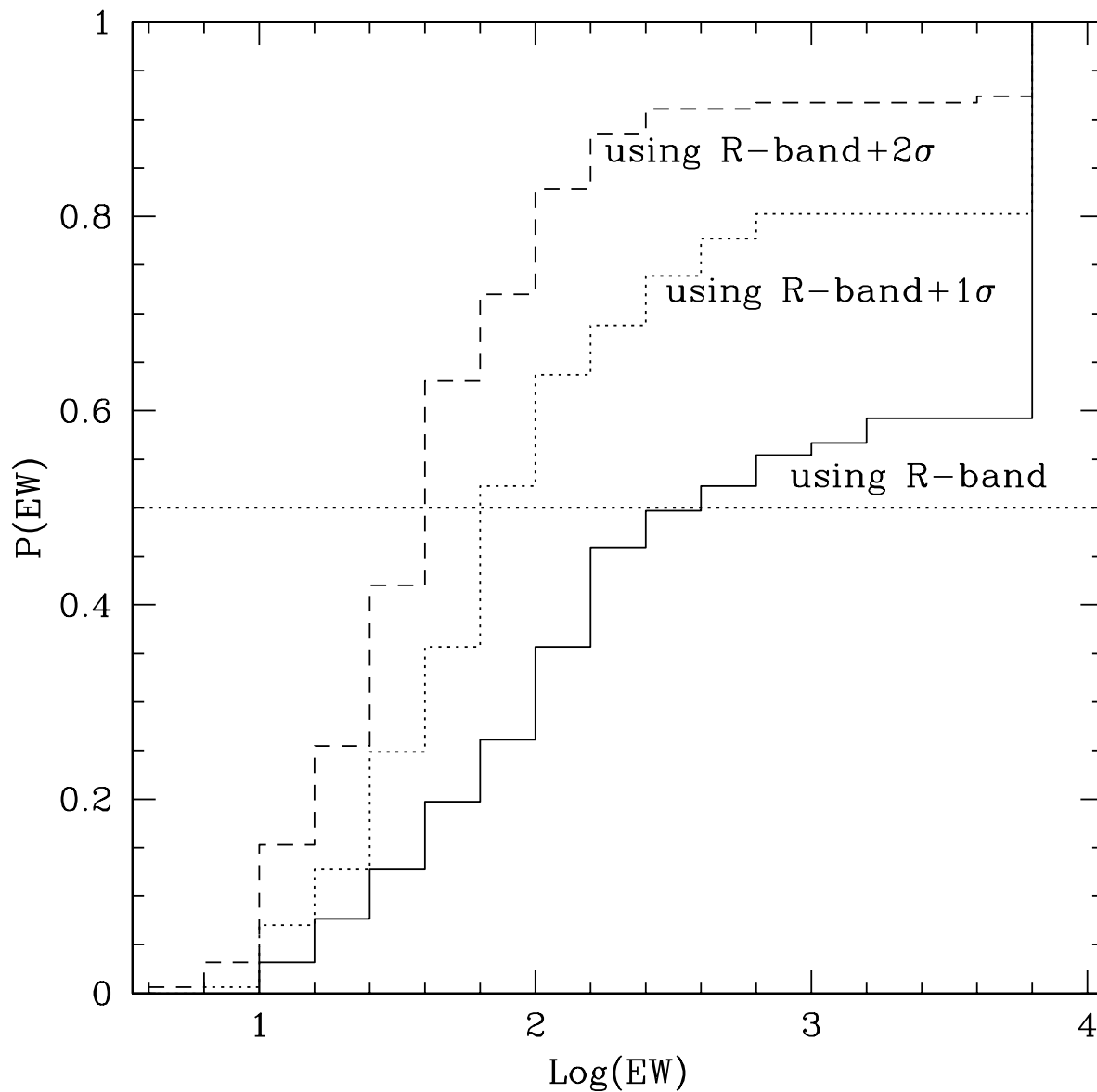


Fig. 1.— The cumulative distribution of Lyman- $\alpha$  equivalent widths in the Lyman- $\alpha$  emitter sample. R-band flux is not detected in about half the sample. The solid line uses measured R-band fluxes to calculate EWs and sources with negative R-band fluxes are placed in the last bin. The dotted and dashed lines show the EWs calculated after adding 1 and 2- $\sigma$  flux to the measured R-band flux. More than 60% of the sources show equivalent widths  $> 240$  Å, the maximum allowed by reasonable stellar population models (Charlot & Fall 1993)

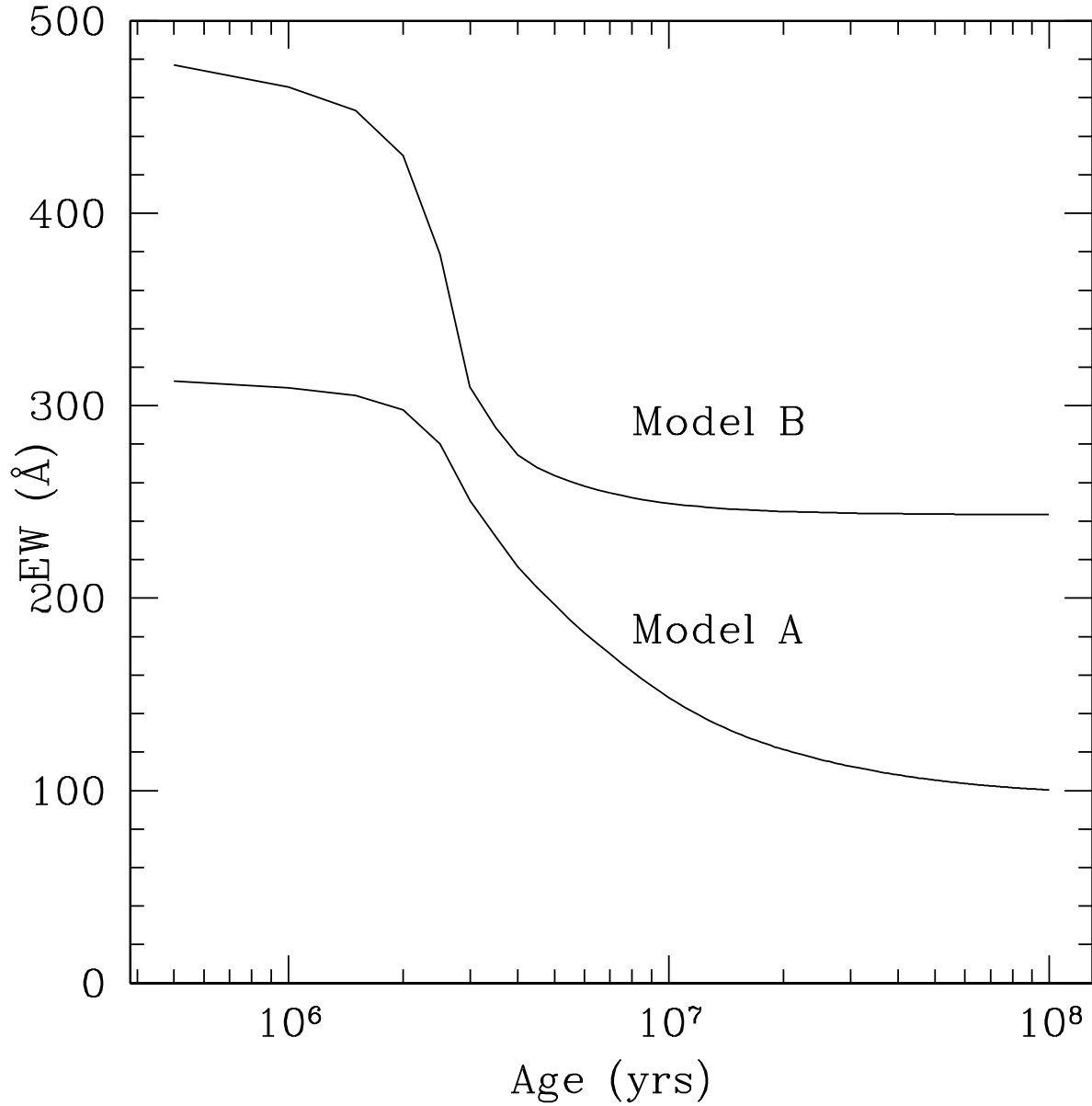


Fig. 2.— The evolution of Lyman- $\alpha$  equivalent width as a function of age for models (A) and (B). Model (C) is assumed to have a similar curve to (A), except that it is normalized to 1122  $\text{\AA}$  at age  $10^6$  years (see text for details).

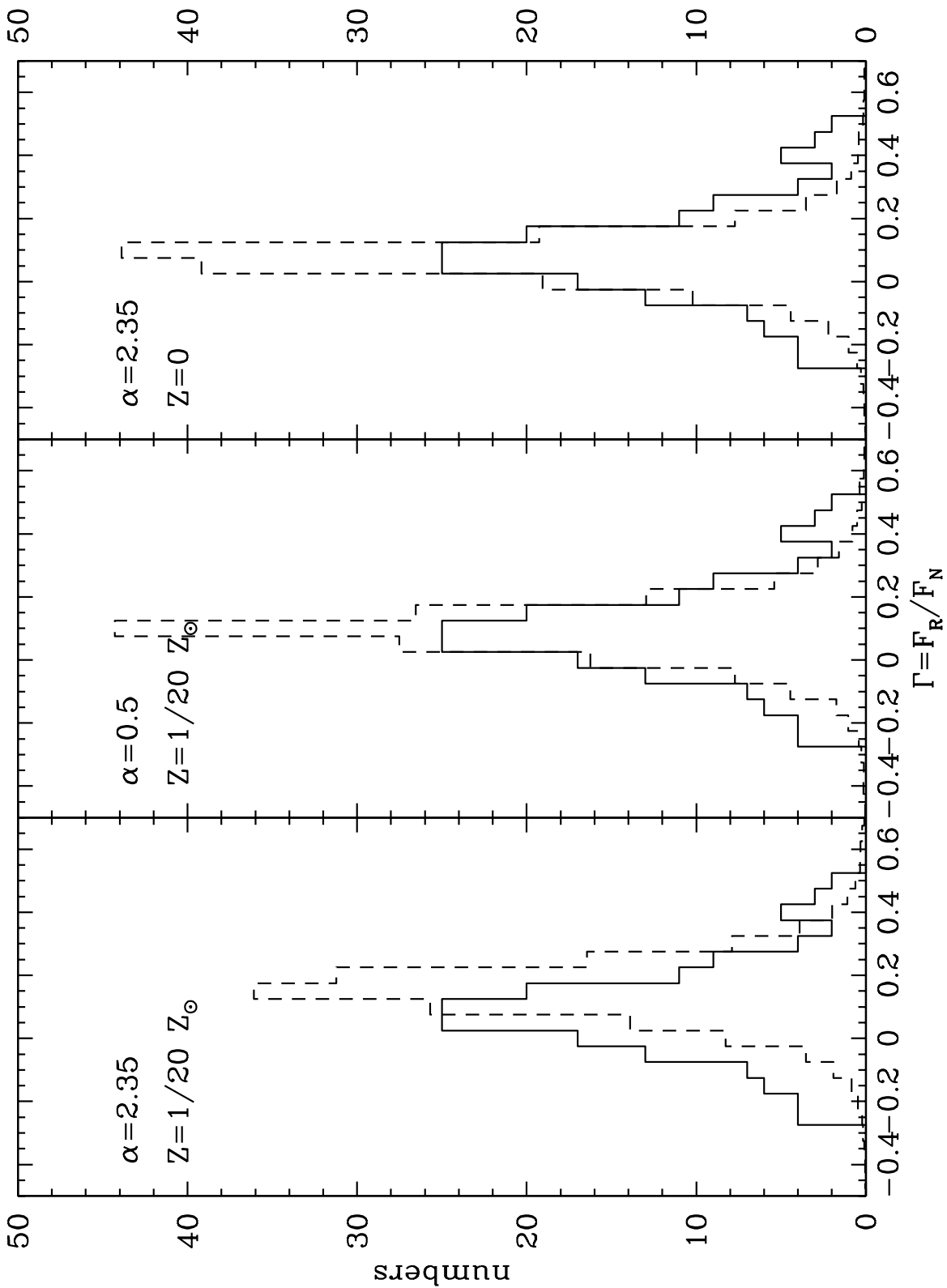


Fig. 3.— The observed distribution (solid histogram) and model distributions (dashed histograms) of the broad band to narrow band flux density ratio  $\Gamma$  are shown for models (A), (B), and (C). The models counts are normalised to match the observed numbers of Lyman- $\alpha$